

## **Robust Image Features: Concentric Contrasting Circles and Their Image Extraction**

*Lance B. Gatrell  
William A. Hoff*

*Cheryl Sklair*

*Advanced Computing Technology  
Martin Marietta Civil Space and Communications Company*

## **Cooperative Intelligent Robotics in Space II**

**William E. Stoney**  
*Chair/Editor*

**12-14 November 1991  
Boston, Massachusetts**

*Sponsored and Published by*  
**SPIE-The International Society for Optical Engineering  
P.O. Box 10, Bellingham, Washington 98227-0010 USA**

**Volume 1612**

**Robust image features:  
Concentric Contrasting Circles and their image extraction**

Lance B. Gatrell, William A. Hoff, Cheryl Sklair

Martin Marietta, M.S. 4372  
Denver, CO 80201

**ABSTRACT**

Many computer vision tasks can be simplified if special image features are placed on the objects to be recognized. A review of special image features that have been used in the past is given, and then a new image feature, the Concentric Contrasting Circle, is presented. The Concentric Contrasting Circle image feature has the advantages that it can be easily manufactured, it is easily extracted from the image, its extraction is robust (true targets are found, while few false targets are found), it is a passive feature, and its centroid is completely invariant to the three translational and one rotational degrees of freedom and nearly invariant to the remaining two rotational degrees of freedom. There are several examples of existing parallel implementations which perform most of the extraction work. Extraction robustness was measured by recording the probability of correct detection and the false alarm rate in a set of images of scenes containing mockups of satellites, fluid couplings, and electrical components. A typical application of Concentric Contrasting Circle features is to place them on modeled objects for monocular pose estimation or object identification. This feature is demonstrated on a visually challenging background of a specular but wrinkled surface similar to a Multi-Layered Insulation spacecraft thermal blanket.

**2. INTRODUCTION**

The ultimate goal of Computer Vision research is to build an autonomous system whose capabilities to recognize and discriminate objects meets or exceeds those of a human. Although significant progress has been made towards this goal, the recognition and pose estimation of arbitrary objects under widely varying lighting conditions and against different backgrounds, all at video update rates, still has not been achieved. Any autonomous robotic system which manipulates and interacts with its environment based on visual sensing must have vision processing capabilities that are robust and fast enough for the task. Examples of tasks requiring robust and fast computer vision capabilities include vision guided robotic manipulation in a factory setting, space based servicing of satellites, space station assembly, and autonomous rendezvous and docking of spacecraft, etc.

To develop a working system now, the typical approach is to constrain the problem sufficiently so that the required processing can be performed on the available hardware at the specified update rates. One such common approach places special/artificial markings on the objects to aid in the recognition and/or pose estimation problem. The problem, then, is how to extract and identify these special markings in the image. Once the special target features have been located and identified, they are used in the simplified object recognition and/or pose estimation solution. Several examples of artificial image features will be given, followed by the introduction of a new, robust, artificial target feature (and its extraction) known as a Concentric Contrasting Circle (CCC). A demonstration of the usefulness of this CCC target feature will be given at the end.

**3. PAST WORK**

There are two general classifications of target features, passive, and active. An active feature is one which changes its appearance in order to be sensed, while a passive feature does not change in appearance during sensing. Likewise, a sensor can be classified as active or passive, depending on whether the sensor changes the scene to perform its sensing.

A common example of special markings as key object features is a *passive*, solid circle. A few of the many examples of using black or white circles can be found in the references<sup>1,2,3</sup>. Colored circles (red, green, blue, yellow, etc.) were also used by Magee<sup>4</sup>. Solid circles are useful when the image scenes are clean, uncluttered, and with known backgrounds. In such circumstances, the targets are assumed to be the only large homogeneous regions with the desired characteristics (ie. black, white, colored, etc.). If the background contains regions with characteristics similar to the target circles, such as background shadows or other dark objects when the target features are black circles, the discrimination of the correct target circles becomes difficult. Two approaches to discriminating circular shapes from arbitrary shapes are the decoupled Hough Transform<sup>5,6</sup>, and the use of the eccentricity of the region from the second order moments. The Hough Transform approach is computationally expensive to compute, and clustering techniques must be used in the Hough space to find the circles. Of course, if the plane

of the circle is not parallel with the image plane, the projected shape of the circle is not invariant--it is an approximate ellipse. Thus, finding circles of arbitrary size and at arbitrary orientations is a difficult problem. Simple solid circles probably should not be used as the target features when the true regions must be discriminated from many other regions of the same size.

LED's are a common form of special markings for real-time object identification and pose estimation. Flashing LED's are *active* image features that can be robustly extracted by image subtraction. Several applications of active flashing LED's are listed by Schneider<sup>7</sup>, and were also used Teitz<sup>8</sup> and Magee<sup>9</sup>. An active (flashing) LED object feature has the disadvantage that the command from the sensor to the object to activate the LED must be transmitted through some medium--typically wire, although radio frequency has also been used. Constantly illuminated, or *passive* LED's, have also been used, but are less reliable since the feature identification constraint is that they are the brightest image points. Several applications that used passive LED's are also listed by Schneider<sup>7</sup>. The disadvantages of LED's are the additional complexity, weight, power, cost, and failure risks. These disadvantages are greater for active LED's than for passive LED's.

Wolfe, et al., in their Robotic Locating System<sup>10</sup>, included the use of reflective tape and retroreflectors as the target feature of interest. These *passive* target features were illuminated by a laser light (an *active* sensor) to produce a high contrast target.

Howard and Dabney describe their development of another specialized object feature and recognition technique using two lasers, optical bandpass filters, and reflective tape<sup>11,12</sup>. The application was a video-based automatic rendezvous and docking system. Their cooperative target consisted of a three-point retro-reflective tape design, adapted from the standard Remote Manipulator System target. The three points are used to compute the relative pose between the two spacecraft for the rendezvous and docking, and so their correct image extraction is critical. A target point is formed from reflective tape with a narrow optical bandpass filter in front, tuned to the second laser's frequency. The optical bandpass filter is necessary to discriminate a target point's reflection from the other reflections off of the highly specular Multi-Layered Insulation (MLI) blankets. Their image feature extraction entails illuminating the passive vehicle with the first laser, then the second laser, and subtracting the two images and finding the centroids of the bright spots in the subtracted images. This system utilizes an *active* sensor and *passive* features. The disadvantage of these markers, though, is the additional system complexity, weight, power, cost, and failure risk of the two lasers and filtered reflective targets.

Another proposed specialized marker is formed by placing ultraviolet sensitive paint on the object, and using an ultraviolet light (*active* sensor) to provide the illumination for the CCD sensor. The targets formed from the ultraviolet paint would be readily apparent in the image. No application of this type of artificial image feature construction is known by the authors.

A new, circular image feature is introduced by Schneider<sup>7</sup>. The intensity of this *passive* image feature varies from black on the perimeter to white in the center, and is shown in Figure 1. Schneider's image targets were initially found by looking for large intensity transitions along a row, computing the intensity weighted centroid of a region of fixed size, and accepting the region as a target if the center was brighter than a threshold, the perimeter edges were darker than a second threshold, and the centroid was "near" the intensity transition. Several "false" targets are initially identified, but usually most are eventually eliminated after failing subsequent feature tests<sup>13</sup>. In Schneider's system, the camera is mounted to the ceiling at a fixed height--so all targets always fill a region of fixed size. The disadvantages of this approach will be manifest when the camera pose relative to the targets has six degrees of freedom. With six degrees of freedom in the camera, the use of a fixed target region size cannot be used.

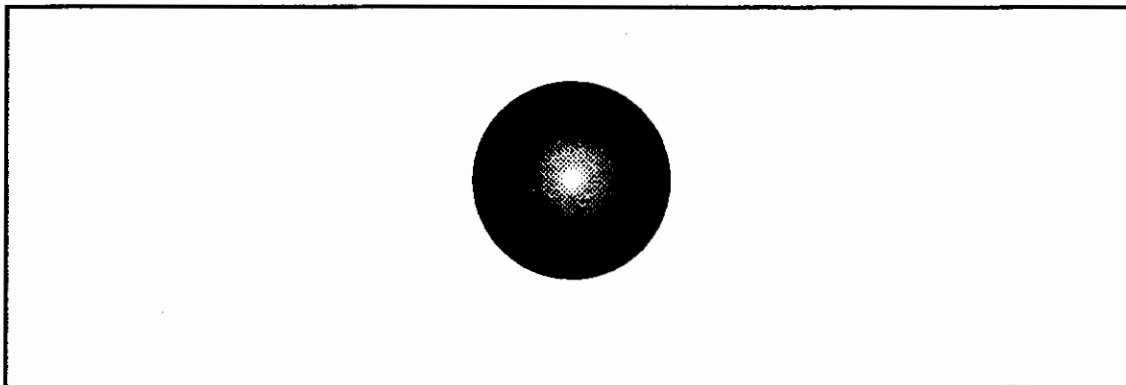
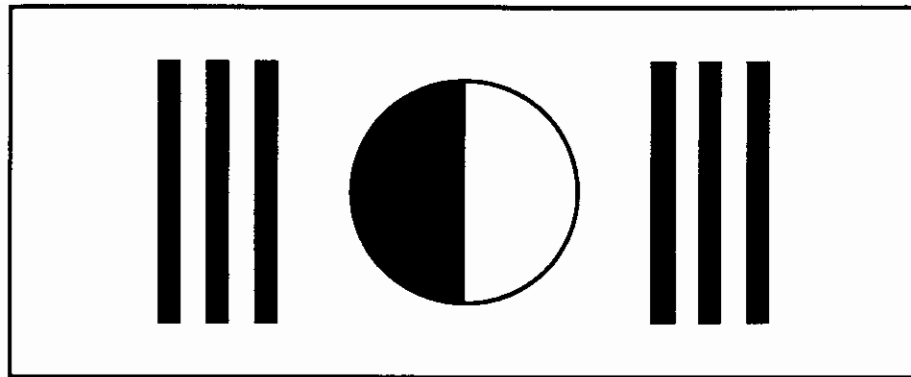


Figure 1. Schneider's intensity-varying image feature.



*Figure 2. Kabuka and Arenas' position target for a mobile robot.*

Kabuka and Arenas developed the use of the *passive* target shown in Figure 2 for mobile autonomous robot position verification<sup>14</sup>. Bar codes on the outside of the target are used for target identification when multiple targets are located throughout the robot's environment. The circle is known to be between the two bar code patterns; the bar codes are found first, and then the circle is found. The projection of the circle is used to compute the pose of the robot. A more complex version of the target suspends the circle in front of the bar code plane. In either case, the image processing outputs that are needed to compute the pose are the lower order moments.

#### 4. CONCENTRIC CONTRASTING CIRCLES

The ideal specialized image feature, then, will be passive so as to minimize system complexity, can be robustly recognized (all true targets are found, while no false targets are found), and its recognition procedure will be computationally simple enough so that the target can be found quickly enough on the available hardware. Out of the passive features discussed so far, solid circles are the least complex. A computationally simple recognition strategy is to threshold the image to produce a binary image, compute the connected component regions, and compute the region centroids, all of which can be done at high speed on commercial-off-the-shelf specialized hardware. However, if solid circles are used in complex, unconstrained scenes, as previously discussed, a more robust recognition strategy must be used than looking for regions with large areas. These factors all led to the development of the Concentric Contrasting Circle as a passive image feature.

A CCC is formed by placing a black ring on a white background. A CCC can also be thought of as a small white circle whose center is coincident with the center of a larger black circle, all on a white background (or vice versa). Since the circles are of contrasting colors and concentric, the designation of Concentric Contrasting Circles was chosen. A CCC is shown in Figure 3.

To produce our CCCs, we draw them using a graphics program such as MacDraw II™ and print them on a laser printer. We have also made CCCs out of name plate stock where the outer black layer is removed by a numerically controlled milling

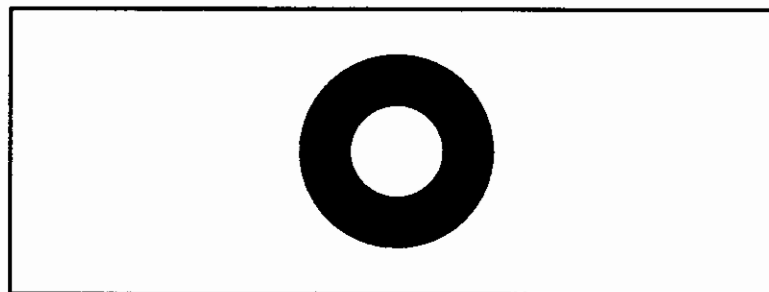


*Figure 3. A Concentric Contrasting Circle.*

machine to expose the lower white layer--the inner circle is just a small black dot stuck on the exposed large white circle. The inner circle does not need to be positioned precisely for this type of target feature since the acceptance criterion is that the centers of the two regions are approximately the same.

#### **4.1. Image extraction**

The power of a CCC is in the robustness and simplicity of its image extraction. To find this image feature, do the following:

1. Segment the image into white regions and black regions.
2. Compute the centroid of every black region and every white region.
3. Take each black region, and compare its centroid to those of the white regions. Each pair of black and white centroids that is equal (within a threshold) is a probable CCC. An alternative approach, assuming that the region segmentation routine produces the hierarchical enclosure of regions within regions, is to only compare the centroids of enclosed regions to a given region.

Although we have found just the simple centroid comparison technique to suffice for most applications, there are additional filtering steps which can be taken to further ensure that the selected features are indeed the desired CCCs. Two checks which can be performed on an individual CCC are:

- compare the ratio of the areas of the two circles to the expected area ratio,
- if the hierarchical enclosure of region information is not available, but the bounding of each region is available, then compare the bounding box of both regions to verify that the color of the inner region is the correct color for the particular target instance.

##### **4.1.1. Extraction Implementation Details**

In our implementation, we have used the simple segmentation techniques of a.) iteratively selecting a global threshold based on the image histogram<sup>15</sup>, b.) performing a binary threshold of the image, and c.) computing the connected components (four neighbor) of the binary image. The use of a global threshold works because the target is formed from the two intensity extremes which are nearly always separated by the automatically selected threshold. The iterative histogram-based threshold selection approach allows the system to find the threshold that is "best" for the particular image lighting and background conditions. Assuming that all pixels in a region are four-connected is a fast and adequate assumption if the regions are thresholded correctly and if the regions do not have narrow (1 pixel wide) connections. The regions produced from a CCC are typically many pixels wide and as such are found by four-neighbor connectedness.

Our Androx ICS-400XM9™ DSP-chip based image processing board performs the digitization, histogram computation, and thresholding. The host Solbourne 4/501 (a Sun SPARC™ compatible 20 MIPS machine) selects the threshold value to use, computes the connected components (the Androx board can also compute the connected components), and compares the centroids to find CCC region pairs. Our current implementation processes an image in 0.8 seconds, and can track four CCC targets simultaneously at 10 Hz.

Our image segmentation approach is very simple, but it works because of the design of the target feature. There are many, more sophisticated, segmentation techniques that could be used if desired, but our experience shows that they typically are not needed.

An advantage of the image extraction simplicity is that the extraction steps can be performed in real time by many of the special purpose image processing boards available today. Some examples of vendors selling hardware that can perform the simple extraction steps outlined above include Data Cube Inc., Aspex Incorporated, Androx, Sharp, Matrox, and Epix etc.

#### **4.2. Invariance to translation and rotation**

The recognition of a CCC is invariant to all six degrees of freedom (DOF)--no matter how you transform the CCC (within the limits of resolution of the lens and CCD), there will still be one region inside of the other. However, as reported by Hoff<sup>16</sup>, the region-based centroid of a circle's projection varies from the projection of the center as a function of image radius and the pan and tilt angles. This is one reason why a centroid equality threshold is used (the other reason being the spatial quantization errors). Using our centroid threshold of 1.5 pixels, a pan angle of 45° (worst angle for centroid errors), and a

radius ratio of two to one, the centroids of the two circles forming the CCC are within the tolerance up to an image radius of 60 pixels for the outer circle. In our experience, we have never needed a CCC of radius 60 pixels in a real application, and have found that we have been able to recognize CCCs in our applications in spite of all transformations that realistically arise.

As mentioned in the previous paragraph, the accuracy of the CCC centroid is only invariant to the three translations and the roll rotation. The centroid accuracy is not invariant to pan and tilt rotations of the circle's plane relative to the camera's coordinate frame. This is not a problem, however, since the centroid errors can be compensated for as explained by Hoff<sup>16</sup>. The net result is that the centroid accuracy of a CCC is effectively invariant to all six DOF.

#### 4.2. Robustness of image extraction

After 18 months of use, we consider the CCC image feature and its extraction to be very robust. Very few false positives (when a CCC was found in the image but no target was there) have been found, and few false negatives (when a CCC was in the image but was not identified) have been reported. The robustness comes from the extremely small probability that two random contrasting intensity regions will have the same centroid by chance, ie. without some geometrical basis for the centroids to align. Although precise statistics on the robustness cannot be given, we did examine forty-two images taken in our robot lab. Sixteen images were taken inside the electronic cages of robotic equipment, sixteen images were taken of three satellite mockups, five images were taken of two different proposed space fluid couplings, and five images were taken of assorted items including robots, a pressure gauge, and a tool box. Figures 4 and 5 show two of the test images containing true positive, false positive, and false negative CCCs. The following information was generated from the test images:

Min Size	Minimum region size (area, in pixels) used in the comparison of the centroid locations. Regions whose area are less than Min Size are ignored. Regions having an area of a few pixels are generally an artifact of the simplistic region segmentation approach we use.
Possible Pairs	Sum, over the forty-two images, of the possible number of pairs of white and black regions that are checked for CCC pairs.
Num True	Number of true CCCs found in the image (true positives).
% True Found	Defined as 'Num True' divided by the actual number of CCCs in the images.
Num False	Number of false CCCs found in the images (false positives).
% False Found	Defined as 'Num False' divided by 'Possible Pairs'.

These statistics are given in Table 1 below.

Twenty-four true CCCs were in the forty-two images described in Table 1. Five of the true CCCs were never located; the reason they were not found was that they were part of a close up target that was viewed from so far away that the black ring was not a complete four-neighbor connected region, as can be seen in Figure 4. As the minimum region size increased, more of the true CCC targets became smaller than the region area threshold, and thus were not considered.

Five of the false positive CCCs listed in the first row of Table 1 have a geometrical basis for their identification; one was a hollow post whose face was highlighted but the inside of the post was not--causing a white ring, one was a black fuse cover with "fuse" written in white letters around the face, one was a bright sticker on the robot with a hole removed from the center,

*Table 1. CCC robustness statistics of forty-two images.*

Min Size	Possible Pairs	Num True	% True Found	Num False	% False Found
8	371152	19	79.2%	13	0.004%
16	152479	19	79.2%	9	0.005%
32	67913	19	79.2%	5	0.007%
64	29474	18	75.0%	2	0.007%
128	13246	16	66.7%	1	0.008%

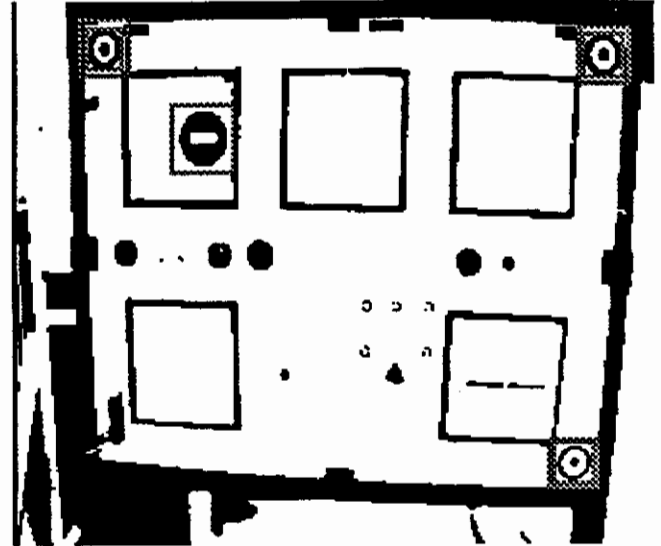
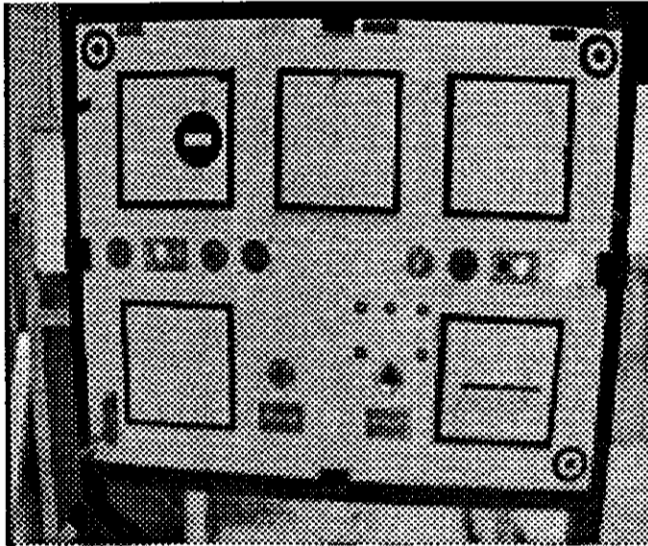


*Figure 4. Multipurpose flat task panel. The raw image is on the left, and the thresholded image is on the right--with overlaid boxes indicating potential CCCs. The three bull's-eye targets in the corners of the task panel are counted twice as true CCCs (once for the smallest black circle inside the white circle, and once for the white circle inside the largest black circle). Five small, true CCCs are below and to the right of the center of the image, but the black rings are too thin to completely enclose the inner white circle, and are thus missed. Notice the white rectangle in the black circle that is marked by a box as a false CCC.*

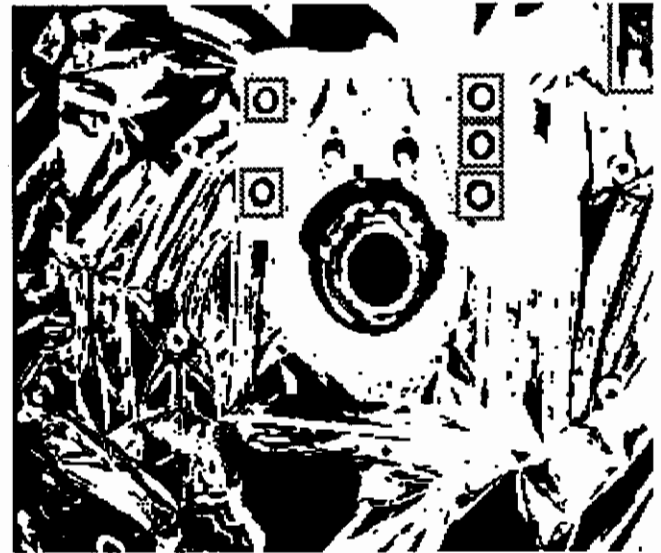
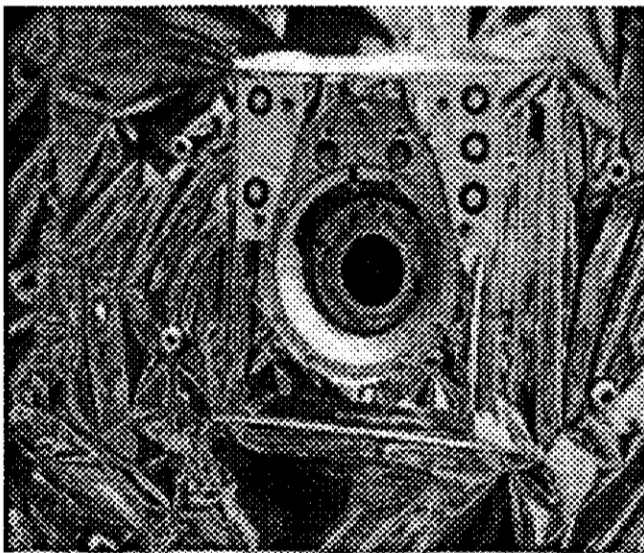


*Figure 5. Refueling receptacle task panel covered with a wrinkled, specular MLI thermal blanket. The raw image is on the left, and the thresholded image is on the right. Five true CCCs are marked by overlaid boxes in the binary image. A false CCC is marked by a box in the upper right corner of the binary image.*

one was the white center grip of a black circular rotating door handle as shown in Figure 4, and one was a highlighted rivet in a darker region. The remaining eight false CCCs were caused by miscellaneous regions--typically formed in a section of the image where the intensity was near the intensity threshold, and thus part of the section was above and part was below the threshold. The false CCC in the upper right corner of Figure 5 is an example of these intensity variations due to the wrinkled, specular nature of the MLI. These CCCs formed from lighting variations are typically small, and are usually not considered because their area is smaller than our normal area threshold of 20 pixels. Using our minimum region size of 20, only seven false negatives were found, three of which had a geometrical basis (hollow post, robot sticker, door handle), and four which were due to intensity variations and other miscellaneous effects.

#### 4.3. Limitations of CCCs

As previously discussed, the accuracy of the computed centroid of a circle is not completely invariant to rotations of the circle's plane out of parallel with the image plane (although the errors can be compensated for). Also, there are practical limits on how small the target may be and how much rotations can be handled. To be recognized, there must always be a connected black ring around a white region. As the viewing distance increases, the width of the black ring shrinks, and will disappear from the image, similarly for the white center circle. Also, as the circle's plane pitches and yaws, the width of the black ring shrinks, and will become lost in the image.

Another limitation of the CCC is that the simple extraction method of matching centroids does not distinguish between concentric circles, concentric squares, concentric triangles, or any other shapes. Any combination of black and white regions may pass the centroid test. If other geometrical shapes of contrasting colors and with common centroids are present in the image, they must be distinguished from the CCCs by the more traditional methods of finding circles or from known 2D or 3D geometrical constraints of the object.

#### 4.4. Other uses of CCCs

Other researchers have used the CCC shape for other purposes. O'Gorman, et al.<sup>17</sup>, computed the edges of each ring of the concentric circles, and basically averaged the locations of the edges in order to improve the accuracy with which the concentric circle could be located. Work by Nielsen<sup>18</sup> used concentric shapes (circles, triangles, etc.) and their areas under perspective transformations to compute all six DOF of the target relative to the camera.

### 5. REPRESENTATIVE USE OF CCC

The Computer Vision IR&D group at Martin Marietta uses CCCs for pose determination of modelled objects. From four coplanar points, all six DOF of the pose of an object can be computed from a single image using a pose estimation algorithm such as Hung-Yeh-Harwood<sup>19</sup>. In our applications, we have added a fifth point to the target pattern--introducing asymmetry which enables unambiguous determination of the target's roll angle. The pose results from our system have been used in teleoperation<sup>20</sup> and autonomous<sup>21</sup> tasks.

Figure 6 shows our Machine Vision Based Teleoperation Aid<sup>20</sup> system in action using the CCC targets shown in Figure 5. As will be recalled, six CCCs were found in Figure 5, of which only five were the true CCCs that formed the target. To eliminate false CCCs, 2D image constraints are applied, which include finding three in a line, and pairs that are on the same side of the line of three CCCs. Groupings of five (three colinear and a pair on the same side of the line of CCCs) are tested to see if they satisfy the 3D constraint of having a valid pose which could project the 3D CCC locations to the given image locations. The false CCC is discarded after the 3D constraint is applied. As seen in Figure 6, cross hairs are overlaid on the four CCC corner targets that are used in the pose computation, and the computed pose is displayed by reticles and text (inches or centimeters, and degrees).

The black reticle on the left is the reference frame for translation errors between the goal location and the current location (left-right, up-down, forward-backward). The white lines originating from the reticle with perpendicular end segments represent the actual translation errors; the operator moves the end effector to make the white lines shrink down to the center of the black translation reticle. In this example, the operator needs to move the end effector left 6.7", up 0.7", and forward 1.0".



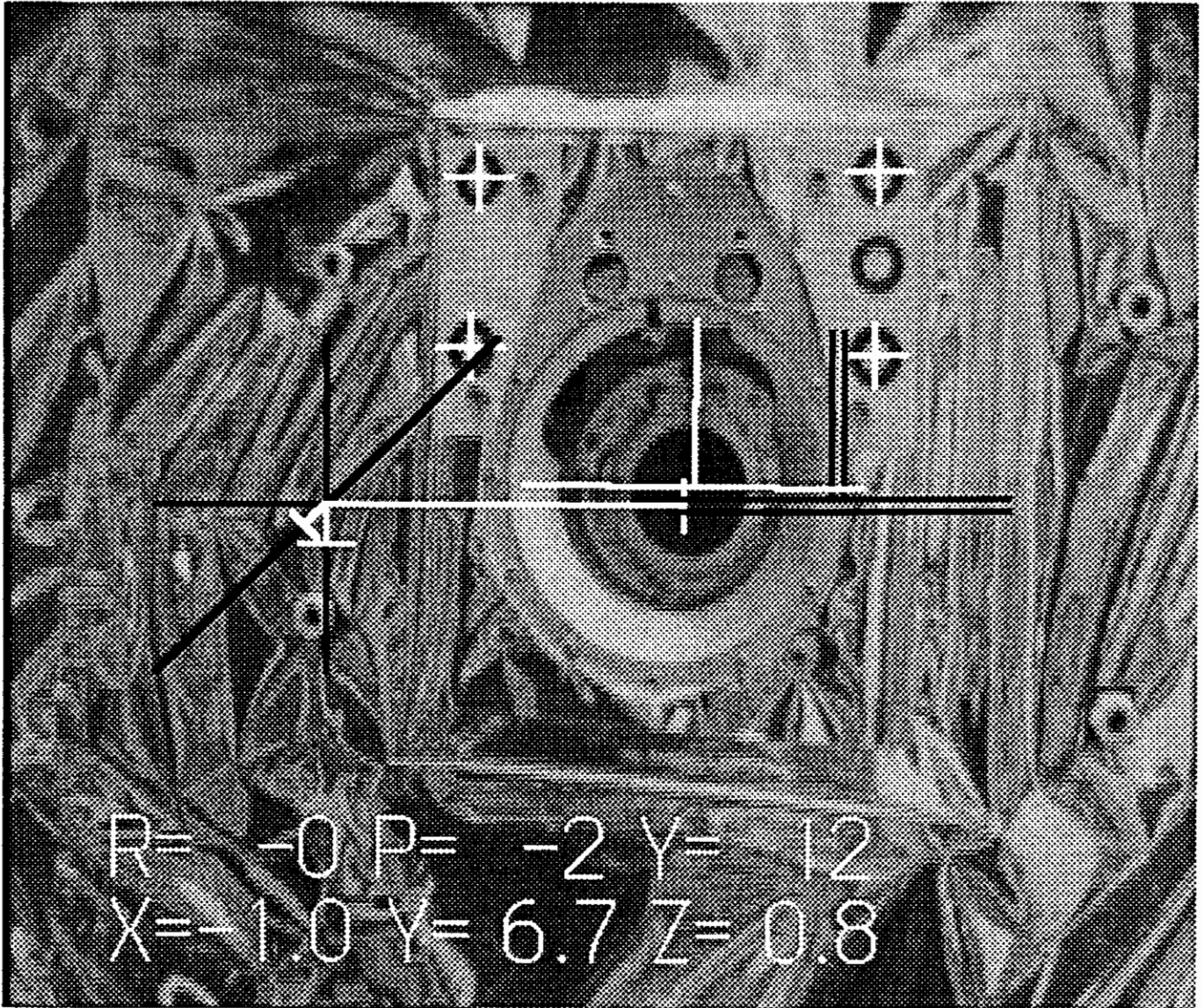


*Figure 6. Machine Vision Based Teleoperation Aid display using Figure 5. The false CCC is eliminated by 2D and 3D geometrical constraints. The pose between the current and desired locations is displayed as graphics and text.*

The black reticle on the right (upside down, hollow T) is the reference frame for orientation errors. The solid white upside-down T represents the current orientation errors. In this example, the operator needs to pitch the end effector down  $2^\circ$ , and yaw  $12^\circ$  to the right (roll orientation is correct to within less than  $1^\circ$ ).

## 6. CONCLUSIONS

There are many tasks where special, artificial markings can be placed on the objects to be recognized or manipulated by an autonomous system. The Concentric Contrasting Circle is a new artificial marking that is very useful for autonomous robot vision systems. The image extraction of Concentric Contrasting Circles is very robust and fast, its recognition is invariant to all six DOF, and the accuracy can be effectively invariant to all six DOF.

## 7. REFERENCES

1. Karin Cornils and Present W. Goode, "Location of Planar Targets in Three Space From Monocular Images," *1987 Goddard Conference on Space Applications of Artificial Intelligence (AI) and Robotics*, May 13-14, 1987.
2. Peter M. Walsh and Larry Shawaga, "Real Time Visual Tracking of Targets in Six Dimensions," *Proceedings, Intelligent Robots and Computer Vision VIII: Systems and Applications*, SPIE vol. 1193, 9-10 November 1989, pp. 94-99.
3. Roger Y. Tsai, "A Versatile Camera Calibration Technique for High-Accuracy 3D Machine Vision Metrology Using Off-the-Shelf TV Cameras and Lenses," *IEEE Journal of Robotics and Automation*, vol. RA-3, no. 4, pp. 323-344, August 1987.
4. Michael Magee, William Hoff, Lance Gatrell, C. Sklair, and William Wolfe, "Employing Sensor Repositioning to Refine Spatial Reasoning in an Industrial Robotic Environment," *International Journal of Applied Intelligence*, Vol. 1, No. 1, July 1991, pp. 69-85.
5. D. H. Ballard, "Generalizing the Hough transform to detect arbitrary shapes," *Pattern Recognition*, vol. 13, no. 2, 1981, pp. 111-122.
6. Xueyin Lin and William G. Wee, "Shape Detection Using Range Data," *1985 IEEE International Conference on Robotics and Automation*, March 25-28, 1985, St. Louis, Missouri.
7. Stanley A. Schneider, *Experiments in the Dynamic and Strategic Control of Cooperating Manipulators*, PhD thesis, Stanford University, Department of Aeronautics and Astronautics, Stanford, CA 94305, September 1989. Also published as SUDAAR 586.
8. T.C. Teitz, "Development of an Autonomous Video Rendezvous and Docking System," Martin Marietta Corporation, NASA Contract No. NAS8-34679, January 1984.
9. Michael Magee, Jeffrey Becker, Donald Mathis, Cheryl Sklair, and William Wolfe, "Multilevel Vision Based Spatial Reasoning for Robotic Tasks," *Proceedings of IEEE International Conference on Robotics and Automation*, 15-18 May 1989, pp. 503-508.
10. William J. Wolfe, Gordon K. White, and Lewis J. Pinson, "A multisensor robotic location system and the camera calibration problem," *Proceedings, Intelligent Robots and Computer Vision*, SPIE Vol. 579, 1985, pp. 420-431.
11. Ricky Howard and Richard Dabney, "Development of a Video-Based Automatic Rendezvous and Docking System," *SME Conference on Robotics in Aerospace Manufacturing*, February, 1989.
12. Richard T. Howard, "Video Based Sensor for Autonomous Docking," *NASA/JSC Autonomous Rendezvous and Docking Conference*, August 15-16, 1990, Houston, Texas.
13. Private communication with Stanley A. Schneider, Department of Aeronautics and Astronautics, Stanford University, Stanford, California, 12 November 1990.
14. Mansur R. Kabuka and Alvaro E. Arenas, "Position Verification of a Mobile Robot Using Standard Pattern," *IEEE Journal of Robotics and Automation*, vol. RA-3, no. 6, December 1987, pp. 505-516.
15. K. V. Mardia and T. J. Hainsworth, "A Spatial Thresholding Method for Image Segmentation," *IEEE Transactions on Pattern Analysis and Machine Intelligence*, vol. 10, no. 6, November 1988, pp. 919-927.
16. William Hoff, Lance Gatrell, Dan Layne, Guy Bruno, and Cheryl Sklair, "Compensating for Centroid Errors Due to Surface Tilt and Lens Distortion," submitted to *IEEE Computer Society Conference on Computer Vision & Pattern Recognition*, to be held June 15-18, 1992, Champaign, IL.
17. Lawrence O'Gorman, Alfred M. Bruckstein, Chinmoy B. Bose, and Israel Amit, "Subpixel Registration Using a Concentric Ring Fiducial," *Proceedings 10th International Conference on Pattern Recognition*, 16-21 June 1990, Volume II, pp. 249-253.

18. Lars Nielsen and Gunnar Sparr, "Perspective area-invariants," *Proceedings 5th Annual Conference on Image Analysis*, pp. 209-216.
19. Yubin Hung, Pen-Shu Yeh, and David Harwood, "Passive Ranging to Known Planar Point Sets," *1985 IEEE International Conference on Robotics and Automation*, March 25-28, 1985, St. Louis, Missouri.
20. W. Hoff, L. Gatrell, and J. Spofford, "Machine Vision Based Teleoperation Aid," *Proc. of Goddard Conf on Space Applications of Artificial Intelligence*, NASA Conference Publication 3110, May 1991, pp. 199-213.
21. M. Morgenthaler, G. Bruno, J. Spofford, R. Greunke, and L. Gatrell, "A Testbed for Tele-Autonomous Operation of Multi-Armed Robotic Servicers in Space," *Proc. of Cooperative Intelligent Robotics in Space*, SPIE Vol. 1387, November 1990, pp. 82-95.